APPLIED ORGANOMETALLIC CHEMISTRY, VOL. 12, 427–433 (1998)

Si/C Phases from the IR Laser-induced Decomposition of Divinylsilane

Vladislav Dřínek[1], Zdeněk Bastl[2], Jan Šubrt[3] & Josef Pola[1],
[1]Institute of Chemical Process Fundamentals, Academy of Sciences of the Czech Republic, 165 02 Prague, Czech Republic
[2]J. Heyrovský Institute of Physical Chemistry, Academy of Sciences of the Czech Republic, 182 23 Prague, Czech Republic
[3]Institute of Inorganic Chemistry, Academy of Sciences of the Czech Republic, 25 068 Řež near Prague, Czech Republic

Transversely excited atmospheric (TEA) CO_2 laser-induced decomposition of divinylsilane in the gas phase yields unsaturated C_2–C_4 hydrocarbons, benzene and vinylsilane, and it represents a convenient process for chemical vapour deposition of thin solid films composed of silicon carbide and polycarbosilane. © **1998 John Wiley & Sons, Ltd.**

Appl. Organometal. Chem. **12**, 427–433 (1998)

Keywords: laser; chemical vapour deposition; thin films; Si/C/H materials; divinylsilane; silicon carbide; polycarbosilane

Received 28 July 1997; accepted 18 November 1997

INTRODUCTION

Hydrogenated amorphous $Si_{1-x}C_x$ films have recently attracted much attention due to their significance in photovoltaic and optoelectronic applications and in high-temperature ceramics. They can be deposited from the gas phase by conventional pyrolysis, photolysis or plasma-assisted decomposition of various hydridocarbosilanes. The composition and therefore the properties of the films are known (see for example Refs 1–4) to be affected by the conditions of chemical vapour deposition (CVD) and by the precursor structure. Regarding the precursors, silacyclobutane,[5–7] 1,3-disilacyclobutane,[6–8] disilylmethane,[9,10] trisilylmethane,[10] 1,3-disilabutane,[11] 1,4-disilabutane,[12] tetramethylsilane[13,14] and monoorganylsilanes[15–17] have been examined.

We have observed that while UV laser photolysis of tetravinylsilane is dominated by molecular expulsion of ethene[18] and leads mainly to elemental silicon, infrared multiphoton decomposition (IRMPD) of tetravinylsilane is controlled by expulsion of ethene and ethyne and it affords a solid deposit composed of elemental silicon and a Si/C/H polymer[19].

In a continuation of our studies of IR and UV laser-induced decompositions of organosilanes for CVD of Si/C/H materials (e.g. Refs 6, 7, 12, 15–23) we report in this paper on the TEA CO_2 laser-induced decomposition of divinylsilane (DVS), which is a more suitable candidate for IRMPD than tetravinylsilane due to its stronger absorption in the region of emission of CO_2 laser.

EXPERIMENTAL

The experiments were carried out in a batch reactor (Fig. 1) and in an IR spectroscopic cell (10 cm long, i.d. 3.6 cm). DVS (57 Torr) was irradiated by a TEA CO_2 laser (P. Hilendarski, Plovdiv University; P(18) line at 945.98 cm^{-1}, pulse energy 0.8 J, incident area 1.8 cm^2). The wavelength and flux were checked by a model 16-A spectrum analyser (Optical Engineering Co.) and by a pyroelectric detector (ml-1 JU, Charles University). In experiments with focused radiation, the laser beam was focused (NaCl lens, focal length 8 cm) at the centre of the reactor and the substrate was kept at temperatures 25 and 120 °C.

Chemical changes induced by the laser radiation were determined in separate experiments in an IR spectroscopic cell of volume equal to that of the reactor. The depletion of DVS was monitored using

* Correspondence to: Josef Pola, Institute of Chemical Process Fundamentals, Academy of Sciences of the Czech Republic, 165 02 Prague, Czech Republic.
Contract/grant sponsor: Academy of Sciences of the Czech Republic; Contract/grant number: A4072509.
E-mail: pola@icpf.cas.cz.

 CCC 0268–2605/98/060427–07 $17.50

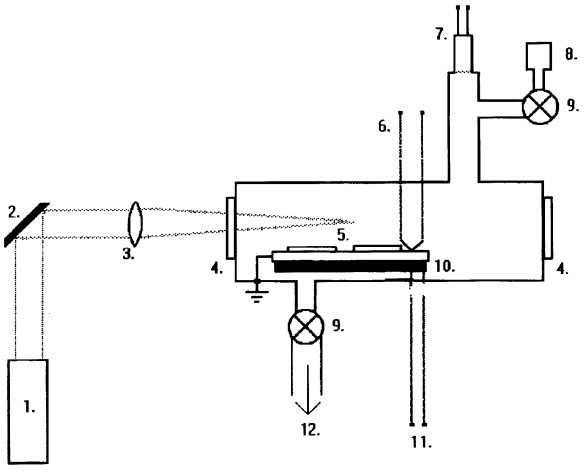

Figure 1 Batch reactor: 1, laser; 2, mirror; 3, NaCl lens (focal length 8 cm); 4, KBr window; 5, substrate; 6, Ni/NiCr thermocouple; 7, pressure gauge; 8, reservoir; 9, valve; 10, substrate heater; 11, substrate heater mains; 12, vacuum.

the diagnostic band at 1407 cm^{-1} and formation of ethene and ethyne was followed at 1887 and 729 cm^{-1}, respectively.

Gaseous products of DVS decomposition were analysed using a Shimadzu QP-1000 mass spectrometer and a GC 14A Shimadzu gas chromatograph (1.5 m column, Porapak P, programmed temperature 20–180 °C). Properties of the films of the material deposited on KBr and Al plates were characterized by means of an FTIR (Nicolet Impact 400) spectrometer, a VG ESCA 3 Mk II electron spectrometer and an SEM Tesla BS 350 ultrahigh-vacuum instrument.

XPS and XAES spectra were obtained using Al Kα radiation ($h\nu$ = 1486.6 eV). The overall energy resolution expressed by the full width of half maximum (fwhm) of the Au $4f_{7/2}$ line was 1.2 eV. The background pressure of residual gases during accumulation of spectra was typically 10^{-6} Pa. The spectra of Si(2*p*), C(1*s*) and O(1*s*) photoelectrons and Si ($KL_{23}L_{23}$) Auger electrons were measured. The peak positions and areas were determined by fitting the unsmoothed experimental data after subtracting nonlinear[24] background. Core-level binding energies were determined with an accuracy $\pm$0.2 eV. Theoretical photoionization cross-sections[25] were used to convert peak areas into the elemental concentrations. For the sake of comparison, XPS and XAES spectra of an authentic sample of silicon carbide (Aldrich Chem. Co., Milwaukee, WI, USA) were also measured.

DVS (99% purity) was prepared by the reported procedure[26] and was distilled and degassed before use.

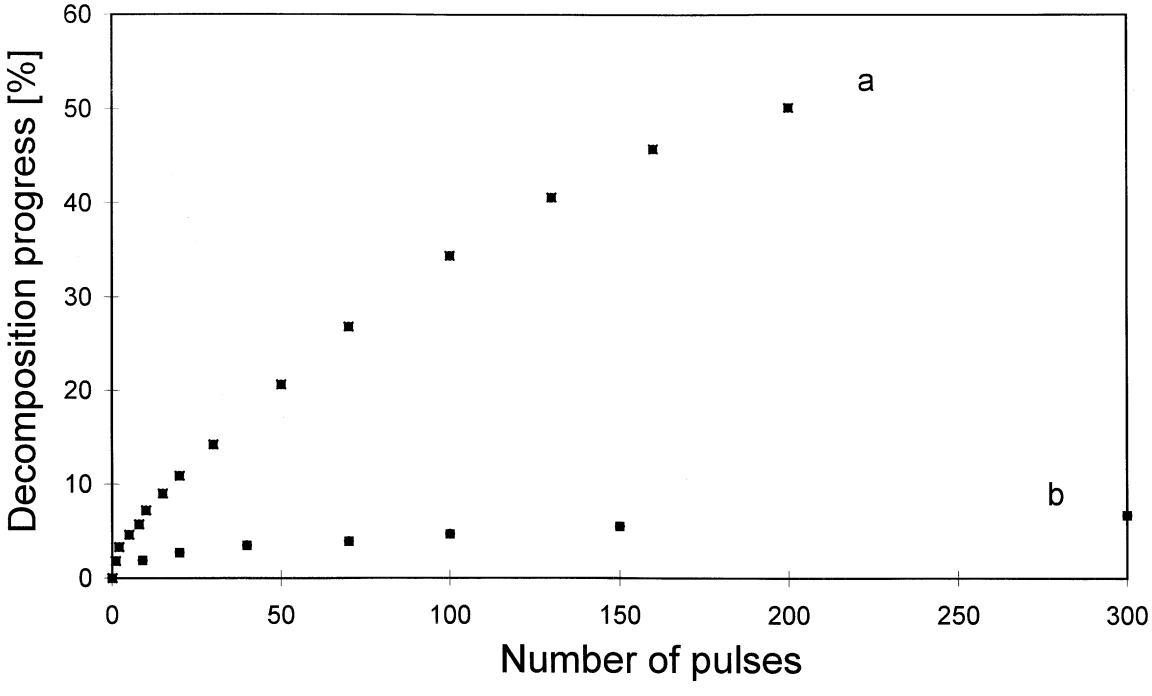

Figure 2 Dependence of the depletion of DVS on the number of pulses, using (a) focused and (b) unfocused radiation.

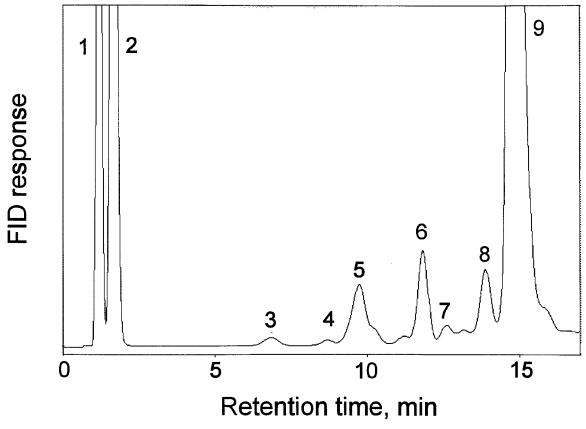

Figure 3 Typical GC trace of gaseous products from IRMPD of DVS. Peak identification: 1, C_2H_4; 2, C_2H_2; 3, $CH_3CH = CH_2$; 4, $H_2C = C = CH_2$; 5, $H_2C = CHSiH_3$; 6, $H_2C = CH\text{-}CH = CH_2$; 7, $H_2C = C\text{-}C \equiv CH$; 8, $HC \equiv C\text{-}C \equiv CH$; 9, DVS.

RESULTS AND DISCUSSION

Irradiation into the absorption band of DVS centred at 943 and 954 cm^{-1} (doublet, σ(Si–H) mode, absorptivity 7.9×10^{-3} cm^{-1}, $Torr^{-1}$ at 946 cm^{-1}) leads to the formation of a multitude of gaseous compounds and the deposition of a solid product. The progress of decomposition is enhanced by focusing the radiation (Fig. 2); thus, for example, 250 pulses of the focused radiation depletes DVS by *ca*. 50%, while the same number of pulses of unfocused radiation leads only to less than 10% depletion. Both types of radiation yield the same gaseous products in very similar quantities; thus at 30–50% conversion the gaseous products are ethene (25–32%), ethyne (50–64%), propene (<1%), propadiene (<0.5%), vinylsilane (5–12%), buta-1,3-diene (2–3%), but-1-en.-3-yne (<0.5%), buta-1,3-diyne (2–4%) and benzene (<1%). A typical GC trace of the mixture of these products is given in Fig. 3.

Gas-phase chemistry

In discussing possible routes operating during IRMPD of DVS, we are guided by primary decomposition modes operating with organosilanes which are 1,1-H_2, 1,2-H_2 and hydrocarbon elimination.[27,28] DVS decomposition has not yet been examined, but structurally similar vinylsilane has been reported[29] to undergo a complex homogeneous decomposition via initial 1,1-H_2, 1,2-H_2 and ethene elimination ($H_3C_2SiH_2SiH_3 \rightarrow H_3C_2(H)Si: + H_2$, $H_3C_2SiH_2SiH_3 \rightarrow H_2C = C =$

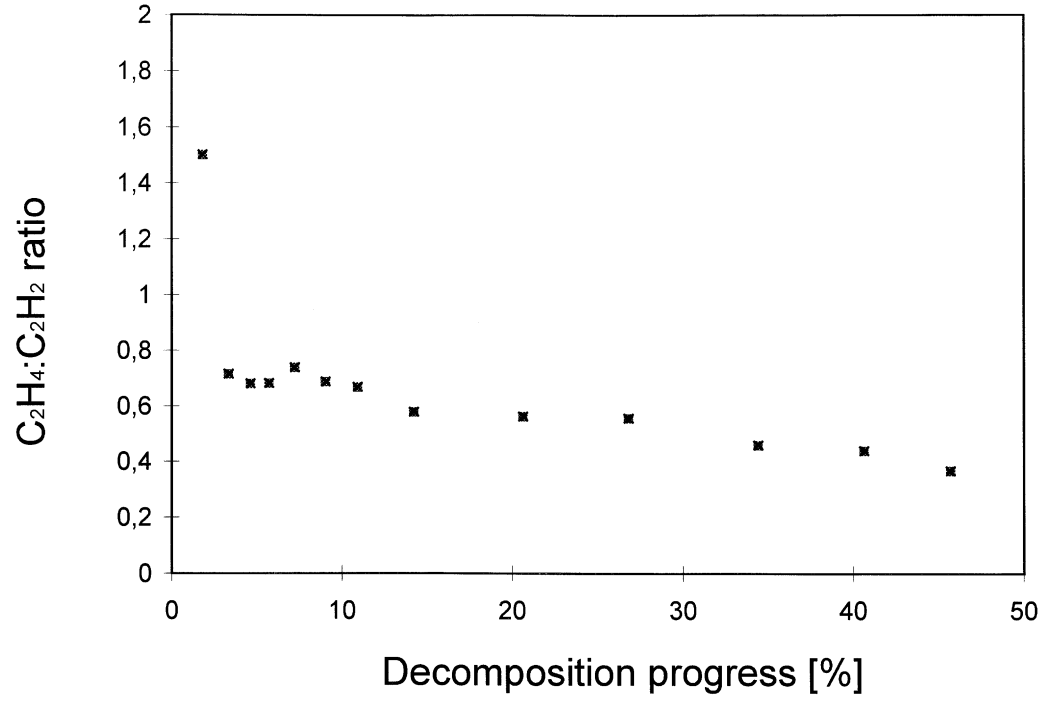

Figure 4 Dependence of the ethene/ethyne ratio on the progress of decomposition.

$SiH_2 + H_2$, and $H_3C_2SiH_2SiH_3 \rightarrow H_2Si: + C_2H_4$, respectively), and via the silylene-chain sequence $H_3C_2(H)Si: \rightarrow C_2H_2 + H_2Si:$, $H_2Si: + H_3C_2SiH_3 \rightarrow H_3C_2SiH_2SiH_3 \rightarrow H_3C_2SiH_2(H)Si: + H_2$, $H_3C_2SiH_2(H)Si: \rightarrow H_3C_2(H)Si: + H_2Si:$.

The three primary steps undoubtedly occur in IRMPD of DVS, too. However, the relative amounts of the gaseous products in the shock-induced thermal decomposition[29] and in our experiments differ. While the amounts of ethene and ethyne in the former decomposition are very similar, those in IRMPD are noticeably in favour of ethyne (Fig. 4). This suggests that the initial 1,1-H_2 elimination (Eqn [1]) and the (similar) silylene chain sequence involving steps [2] and [3] and affording ethyne are more strongly preferred in IRMPD of DVS.

$$DVS \rightarrow (H_2C = CH)_2Si: + H_2 \qquad [1]$$

$$(H_2C = CH)_2Si: \rightarrow (H_2C = CH)HSi: + C_2H_2 \qquad [2]$$

$$(H_2C = CH)HSi: \rightarrow H_2Si: + C_2H_2 \qquad [3]$$

Significant formation of ethene is in accord with the occurrence of the alkene elimination pathway (Eqn [4]).

$$DVS \rightarrow (H_2C = CH)HSi: + C_2H_4 \qquad [4]$$

The C_4 hydrocarbons, being observed only in very small yields, make us believe that the role of homolytic Si–C cleavage into a H_2C = CH radical is not important. This assumption is in line with the observation of very small yields of buta-1,3-diene and with the known fact that combination of small radicals is preferred over their disproportionation.[30] (We assume that the $C_2H_3^{\bullet}$ radical is mostly involved in hydrogen abstraction from DVS, since abstraction of H(Si) by radicals is favoured over radical combination and disproportionation[31]).

Characterization of the deposits

IR absorption spectra of the solid films typically show a strong band at 810 cm^{-1} with a shoulder at 860 cm^{-1} as well as weak bands at 580, 650 and 700 cm^{-1}. Due to the lack of bands at ≈2100 (ν_{Si-H}) and 2900 (ν_{C-H}) cm^{-1}, these are mostly assignable to ν_{Si-C} vibrations. This IR spectral pattern confirms that the content of hydrogen in the films is very low.

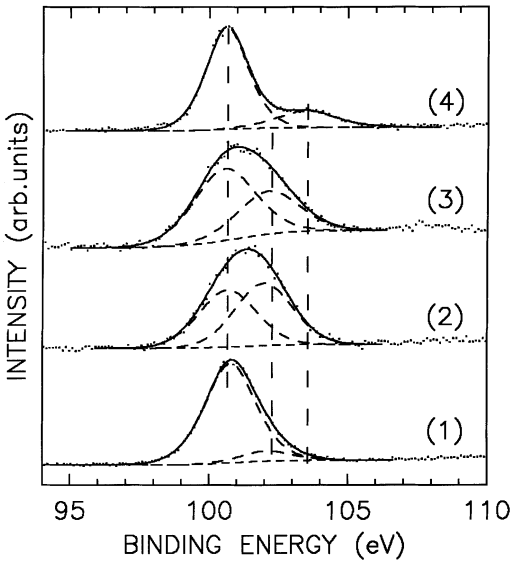

Figure 5 Fitted Si(2*p*) photoelectron spectra of (1) the deposit obtained at ambient temperature; (2) the deposit obtained at 120 °C; (3) the same deposit after mild Ar-ion sputtering; and (4) an authentic sample of SiC.

The measured core-level binding energies and calculated values of the modified Auger parameter (defined as the sum of the binding energy of the Si(2*p*) photoelectrons and the kinetic energy of the Si($KL_{23}L_{23}$) Auger electrons[32]), along with assign-

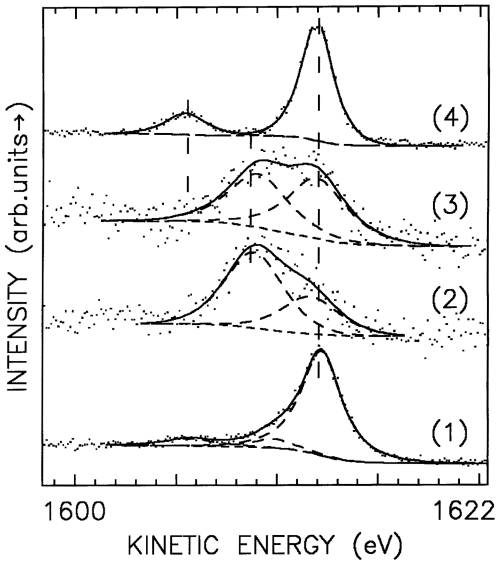

Figure 6 Fitted spectra of Si($KL_{23}L_{23}$) Auger electrons. Definitions as in Fig. 5.

Table 1 The Si(2*p*) and C(1*s*) core-level binding energies (eV) of the fitted photoemission lines, their assignments, the Si Auger parameter, α(eV), surface stoichiometry of the samples (normalized to Σ Si = 1) and content of Si carbide (% of Si)

Sample[a]	Si(2*p*)	Assignment	C(1*s*)	Assignment	α	Overall surface stoichiometry	Carbide content
1	100.7	Si carbide	283.5	Carbide	1714.8	$Si_{1.00}C_{1.55}O_{0.38}$	90
	102.1	Si polymer	284.8	Polymer and hydrocarbons	1713.7		
2	100.7	Si carbide	283.3	Carbide	1714.7	$Si_{1.00}C_{3.93}O_{2.25}$	47
	102.0	Si polymer	284.7	Polymer	1712.2		
			286.4	-C-O-groups			
			288.8	Carboxylic groups			
3	100.5	Si carbide	283.4	Carbide	1714.1	$Si_{1.00}C_{1.95}O_{0.70}$	57
	102.1	Si polymer	284.8	Polymer and hydrocarbons	1712.7		
4	100.6	Si carbide	282.7	Carbide	1714.2	$Si_{1.0}C_{1.32}O_{0.65}$	
	103.5	Si oxide	285.0	Hydrocarbon contamination			82
			286.3	-C-O-groups			
			289.1	Carboxylic groups			

[a] The samples were obtained as follows: (1) deposition at ambient temperature; (2) deposition at 120 °C; (3) ion sputtering of sample 2 using Ar ions with energy 5 keV (I = 20 μA, t = 5 min); (4) silicon carbide (Aldrich).

ments and stoichiometry of the superficial layers of the samples under study, are summarized in Table 1. The Si(2*p*) spectra of the deposits (Fig. 5) reveal the presence of two components which are more clearly seen in the Si($KL_{23}L_{23}$) spectra (Fig. 6). They are consistent with presence of the two different chemical states of Si, namely silicon carbide and silicon, in the Si/C/H polymer. (With an authentic SiC sample peak at 103.5 eV comes from silicon oxides, present on the sample surface.) The value of the Auger parameter obtained, 1714.45 ± 0.35 eV, is characteristic of silicon carbide.[32,33] The carbidic C(1*s*) component (Fig. 7) in the deposits is shifted by 0.7 eV to a higher binding energy, compared with the authentic sample of SiC. In analogy with some other carbonaceous materials (see e.g. Ref.[34]), we explain this shift as a consequence of the amorphous structure of the deposits. It follows from comparison of the results obtained with samples 2 and 3 that adsorption of gaseous products and precursor on the surface of the deposit is very likely. After removal of the sample from the reactor, some of the adsorbed species can react further with ambient atmosphere. The surface species formed by the above processes can be removed by mild argon-ion sputtering.

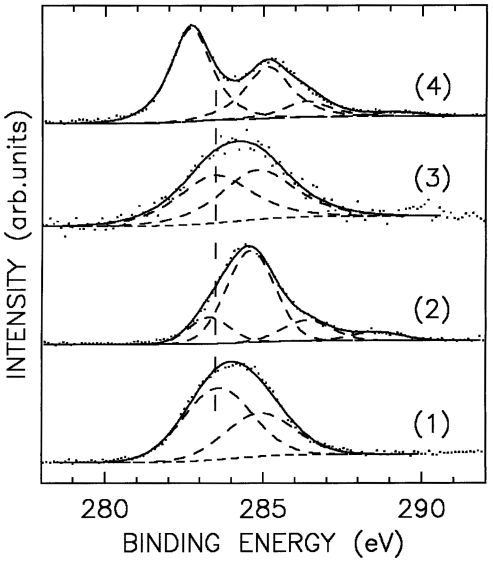

Figure 7 Fitted photoelectron spectra of C(1*s*) electrons. Definitions as in Fig. 5.

We note that incorporation of oxygen into the superficial layers of the IR laser-deposited films upon their exposure to the atmosphere is a common phenomenon (see, e.g., Refs 6, 12 and 15) and can be attributed to residual reactivity of solid agglomerates due to some Si = C bond content.

SEM images of the deposits (Fig. 8) show that the deposits have a particulate structure and consist of agglomerates whose size is larger than 10 μm. The larger magnification in Fig. 8(a) reveals that these agglomerates are bonded together, which suggests that the particles show some degree of reactivity and react, after deposition on the substrate, to increase their size. Although it is difficult to be specific at present, we judge that the reactions involved are insertion of silylenes into the Si–H bonds and polymerization on C = C and Si = C bonds.

The films obtained in this work differ in

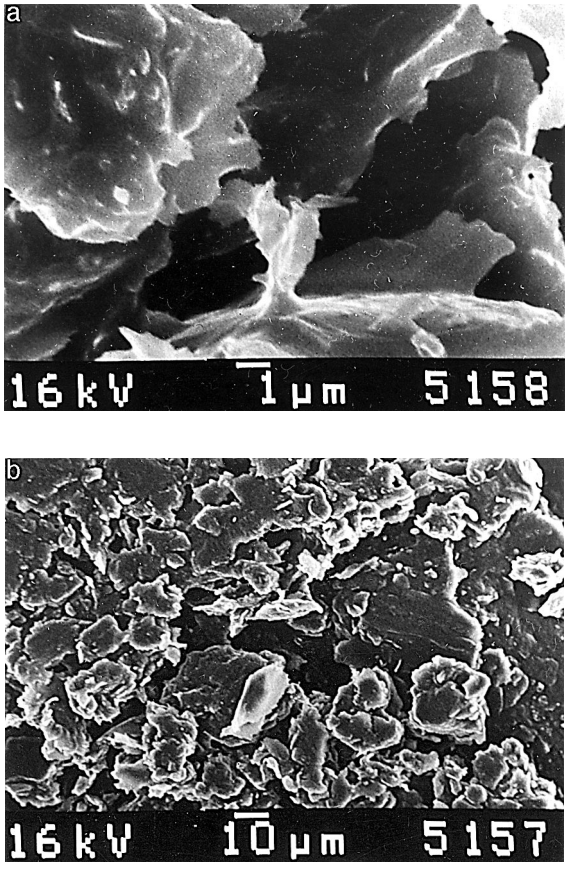

Figure 8 SEM of the film deposited on substrate kept at ambient temperature.

composition from the others prepared from single precursors by laser-induced CVD. The deposition of pure silicon carbide by IR laser heating of a suitable precursor in the gas phase on a substrate at ambient temperature is, in principle, a very intriguing technique. However, much effort devoted to that objective has not been completely successful. Our studies have shown that the interaction of some organosilanes (silacyclobutane,[6] 1,3-disilacyclobutane,[6] 2-chloroethenylsilane[15]) with unfocused (low-flux) pulsed IR laser radiation yields Si/C/H phases which are mainly polycarbosilanes and in which silicon carbide is only a minor constituent. On the other hand, focused (high-flux) laser radiation interacting with the same compounds affords mostly silicon carbide along with a minor portion of polycarbosilanes.[6,15] Focused radiation interacting with tetravinylsilane[19] and 1,4-disilabutane[12] affords materials composed of elemental silicon and polycarbosilane, and SiC, polycarbosilane and Si, respectively. The same type of radiation absorbed in 2-propenylsilane[17] yields phases composed of SiC (major constituent) and polycarbosilane. The most efficient (note—explosive) formation of SiC takes place upon focused irradiation of ethynylsilane.[17] We remark that SiC was also produced as a major constituent by IRMPD of tetramethylsilane.[13] In contrast, UV laser photolysis of mono-organylsilanes results in deposition of almost exclusively saturated polycarbosilanes.[7,16]

CONCLUSION

TEA CO_2 laser-induced decomposition of DVS is an efficient method for depositing thin layers of Si/C/H phases which are composed of silicon carbide (major constituent) and polycarbosilane (minor constituent). It can be inferred that the important decomposition pathways involved in the DVS decomposition are extrusion of ethene and ethyne. The superficial layers of the deposited coatings are sensitive to air and they incorporate oxygen.

Acknowledgment This work was supported by the Grant Agency of the Academy of Sciences of the Czech Republic (grant no. A4072509).

REFERENCES

1. A. E. Kaloyeras, J. W. Corbett, P. J. Toscano and R. B. Rizk, *Mater. Res. Soc. Symp. Proc.* **192**, 601 (1990).
2. A. Figueras, S. Garelik, J. Santiso, R. Rodriguez-Clemente, B. Armas and C. Combescure, *Mater. Sci. Eng. B* 1183 (1992).
3. J. A. O'Neil, M. Horsburg, J. Tann, K. J. Grant and G. L. Paul, *J. Am. Ceram. Soc.* **72**, 1130 (1989).
4. J. M. Agullo, F. Fau-Canillac and F. Maury, *J. Mater. Chem.* **4**, 695 (1994).
5. A. D. Johnson, J. Perrin, J. A. Mucha and D. E. Ibbotson, *J. Phys. Chem.* **97**, 12937 (1993).
6. Z. Bastl, H. Bürger, R. Fajgar, D. Pokorná, J. Pola, M. Senzlober, J. Šubrt and M. Urbanová, *Appl. Organometal. Chem.* **10**, 83 (1996).
7. J. Pola, Z. Bastl, J. Šubrt and R. Taylor, *J. Mater. Chem.* **5**, 1345 (1995).
8. D. J. Larkin and L. V. Interrante, *Chem. Mater.* **4**, 22 (1992).
9. W. Beyer, R. Hager, H. Schmidbaur and G. Winterling, *Appl. Phys. Lett.* **54**, 1666 (1989).
10. H. Schmidbaur, R. Hager and J. Zech, in *Frontiers of Organosilicon Chemistry*, Bassindale, A. R. and Gaspar, P.

P. (eds), The Royal Society of Chemistry, Cambridge (1991), p. 62.
11. J.-H. Boo, K.-S. Yu, Y. Kim, S. H. Yeon and I. N. Jung, *Chem. Mater.* **7**, 694 (1995).
12. E. A. Volnina, J. Kupčík, Z. Bastl, J. Šubrt, L. Gusel'nikov and J. Pola, *J. Mater. Chem.* **7**, 637 (1997).
13. V. M. Scholz, W. Fuss and K.-L. Kompa, *Adv. Mater.* **5**, 38 (1993).
14. S. W. Rynders, A. Scheeline and P. W. Bohn, *J. Appl. Phys.* **69**, 2951 (1991).
15. M. Santos, L. Díaz, Z. Bastl, V. Hulínský, M. Urbanová, J. Vítek and J. Pola, *J. Mater. Chem.* **6**, 975 (1996).
16. J. Pola, Z. Bastl, J. Šubrt, J. R. Abeysinghe and R. Taylor, *J. Mater. Chem.* **6**, 155 (1996).
17. J. Pola, J. Vítek, Z. Bastl, M. Urbanová, J. Šubrt and R. Taylor, *J. Mater. Chem.* **7**, 1415 (1997).
18. J. Pola and R. Taylor, *J. Organometal. Chem.* **489**, C9 (1995).
19. V. Dřínek, Z. Bastl, J. Šubrt, R. Taylor and J. Pola, *J. Anal. Appl. Pyrol.* **35**, 199 (1995).
20. J. Pola, *Radiat. Phys. Chem.* **49**, 151 (1997).
21. J. Pola, *Surface & Coating Technol.* in press.
22. V. Dřínek, Z. Bastl, J. Šubrt, M. Urbanová and J. Pola, *SPIE (Int. Soc. Opt. Eng.)* **2461**, 163 (1994).
23. M. Jakoubková, Z. Bastl, J. Šubrt, D. Čukanová, R. Fajgar and J. Pola, *SPIE (Int. Soc. Opt. Eng.)* **2461**, 121 (1994).
24. D. A. Shirley, *Phys. Rev.* **B5**, 4709 (1972).
25. I. M. Band, Zu. I. Kharitonov and M. B. Trzhaskovskaya, *Atomic Data and Nuclear Data Tables* **23**, 443 (1979).
26. R. J. P. Corriu, C. Guérin, B. J. L. Henner and Q. Wang, *Organometallics* **10**, 3574 (1991).
27. J. Dzarnoski, H. E. O'Neal and M. A. Ring, *J. Am. Chem. Soc.* **103**, 5740 (1981).
28. B. A. Sawrey, H. E. O'Neal, M. A. Ring and D. Coffey, *Int. J. Chem. Kinet.* **16**, 289 (1984).
29. S. F. Rickborn, M. A. Ring, H. E. O'Neal and D. Coffey, *Int. J. Chem. Kinet.* **16**, 289 (1984).
30. M. J. Gibian and R. C. Corley, *Chem. Rev.* **73**, 441 (1973).
31. M. Ballestri, C. Chatgilialoglu, M. Guerra, A. Guerrini, M. Lucarini and G. Seconi, *J. Chem. Soc., Perkin Trans. 2* 421 (1993).
32. D. Briggs and M. P. Seah (eds), *Practical Surface Analysis*, Vol 1, *Auger and X-ray Photoelectron Spectroscopy*. Wiley, Chichester, 1990, p. 587.
33. *NIST X-ray Photoelectron Spectroscopy Database*, US Dept of Commerce, Gaithersburg, 1989.
34. Z. Bastl, *Coll. Czech. Chem. Commun.* **60**, 383 (1995).

